9-2004

Analysis of Adsorbed Contaminants of CaF/sub 2/ Surfaces by Infrared Laser Induced Desorption

JinMei Fu
Florida State University

Yamini Surapaneni
Florida State University

Susan D. Allen
Arkansas State University, allens17@erau.edu

Analysis of adsorbed contaminants of CaF_2 surfaces by infrared laser induced desorption

JinMei Fu[a)]
Department of Chemistry and Biochemistry, Florida State University, Tallahassee, Florida 32306

Yamini Surapaneni
Department Electrical and Computer Engineering, FAMU/FSU College of Engineering, Tallahassee, Florida 32310

Susan D. Allen
Department of Chemistry and Physics and College of Engineering, Arkansas State University, State University, Arkansas 72467

(Received 14 August 2003; accepted 17 May 2004; published 24 September 2004)

157 nm photolithography technologies are currently under development and have been accepted as the leading candidate for fabrication of the next generation semiconductor devices after 193 nm. At this and shorter wavelengths, molecular contamination of surfaces becomes a serious problem as almost all molecules absorb at 157 nm and below. The light transmitted by a photolithographic tool can be significantly decreased by the presence of a few monolayers adsorbed on its many optical surfaces. We have developed a laser induced desorption, electron impact ionization, time-of-flight mass spectrometer (LID TOFMS) to study contaminants on 157 nm and other ultraviolet optics, e.g., polished CaF_2. The LID TOFMS of CaF_2 (100) samples showed water ions, hydrocarbon ions, oxygen-containing hydrocarbon ions, as well as alkali metal ions (Na^+,K^+). For multiple irradiations of one site at fixed laser fluence, the ion intensities decreased as the number of pulses increased, suggesting that surface contaminants were being removed. A degenerate threshold model that assumes preferential adsorption at surface defects was employed to quantitatively analyze the LID data. Desorption thresholds for water and hydrocarbons were obtained from this model. © *2004 American Vacuum Society*. [DOI: 10.1116/1.1772374]

I. INTRODUCTION

Contamination of optical surfaces in a state-of-the-art photolithographic stepper tool has always resulted in reduced device yield if the contamination was sufficiently severe.[1,2] Contaminants can be divided into two types: molecular and particulate. The main focus of the semiconductor industry to date has been the elimination of particulate contamination. Molecular contamination has not been a serious problem at 248 and 193 nm photolithography as it is possible to remove enough molecular contamination using appropriate solvent cleaning techniques, that significant amounts of light will not be absorbed. 157 nm photolithography technology is currently under development for fabrication of the next generation of semiconductor devices after 193 nm. Cleaning by solvents will not be effective at 157 nm because all solvents, including water, absorb strongly at this wavelength. Adsorption of contaminants from ambient atmosphere was also observed on antireflection coatings and high reflectors,[3] as well as on calcium fluoride (CaF_2) surfaces.[4] As an example, a comparison of energy loss at 157, 193, and 248 nm from surfaces having a resident 1 nm water layer on each one is shown in Table I. The energy loss caused by these 1 nm water layers on the surfaces is negligible at 193 and 248 nm, while the loss is very significant at 157 nm. The main candidate material for transmissive optics at 157 nm is CaF_2.[3] Therefore, investigation of adsorbed contaminants on CaF_2 surfaces prepared in a manner similar to that for actual photolithographic stepper optics becomes very important.

While laser cleaning of particles has been studied intensively[1,2,6,7] and shows great efficacy, there are few reports on laser cleaning of molecular contaminants. Measurements at MIT Lincoln Lab (Lexington, MA) showed laser cleaning/removal of surface impurities by observing an initial transmission increase during 157 nm irradiation.[8] A photoinduced cleaning of CaF_2 substrates was investigated using a 157 nm laser source in combination with trace levels of oxygen in the purge gas and shown to be an effective tool for removal of organic contaminants on CaF_2 substrates.[9] Reports from another group suggested that an ultra high vacuum environment is necessary for laser induced desorption due to the readsorption of the desorbed material in ambient atmosphere.[10] Allen *et al.*[11] studied laser induced desorption of water on chemically etched CaF_2 using a quadrupole mass analyzer and found that laser cleaned CaF_2 surfaces did not readsorb water at room temperature under UHV conditions.

In the current work, contaminants on CaF_2 surfaces were analyzed using a laser induced desorption (LID), electron impact (EI) ionization, time-of-flight mass spectrometer (TOF-MS). An Er:YAG laser (2.94 μm) was used because water (a known contaminant on CaF_2) has a strong absorp-

a)Author to whom all correspondence should be addressed; present address: National High Magnetic Field Laboratory, 1800 East Paul Dirac Dr, Tallahassee, FL 32310; electronic mail: jfu@chem.fsu.edu

TABLE I. Energy loss at surfaces with 1 nm water layer at 157, 193, and 248 nm.

Wavelength (nm)	Absorption coefficient of water[5] (cm^{-1})	Energy loss after 1 surface (%)	Energy loss after 10 surfaces (%)
157	1.73×10^{5}	1.7	16
193	1.63×10^{-1}	1.7×10^{-6}	1.6×10^{-5}
248	4.81×10^{-3}	4.8×10^{-8}	4.8×10^{-7}

tion band at this wavelength[12] and photochemical reactions and surface damage are minimized. An electron beam was chosen for postdesorption ionization because almost all molecules can be ionized by EI and it is cost effective. A major advantage of TOF-MS over previous LID experiments is that it can measure all of the desorbed molecules from a single laser shot.

II. EXPERIMENT

The LID experiments were performed using an in house designed LID-EI-TOF apparatus (Fig. 1), which is discussed in detail elsewhere.[13] The desorption laser source is a Q-switched Er:YAG laser (LaserSight Technologies, Inc., formerly Schwartz ElectroOptics Inc., Orlando, FL) operated at a 2 Hz repetition rate with laser pulse width of approximately 100 ns (full width at half maximum). The laser wavelength is 2.94 μm and the maximum output energy is 20 ± 1 mJ/pulse. An intracavity aperture was installed for TEM_{00} mode operation. The beam profile was measured by a pyroelectric camera (Pyrocam II, Spiricon, Inc., Logan, UT) and a gaussian beam profile was confirmed. The incident angle of the desorption laser is 60° from the sample normal and the laser energy is adjusted by varying the number of 1-mm-thick glass filters inserted into the beam path. The transmission of each glass filter is 78%–80% at $\lambda=2.94$ μm. The laser was focused on the sample by a spherical lens ($f=150$ mm) producing a spot size of approximately 360 μm ($D_{1/e}$). Positioning of the laser beam on the 12 mm diameter sample was aided by a He–Ne laser, collinear with the desorption laser, and an ultra-high vacuum (UHV) compatible long working distance microscope. An electronic shutter was placed in the beam path to select single laser pulses on demand, with a time interval between two consecutive pulses >3 s, to eliminate residual heating effects from the previous pulse.[14] The opening time of the shutter was set so that only one laser pulse was allowed to pass for each external trigger pulse.

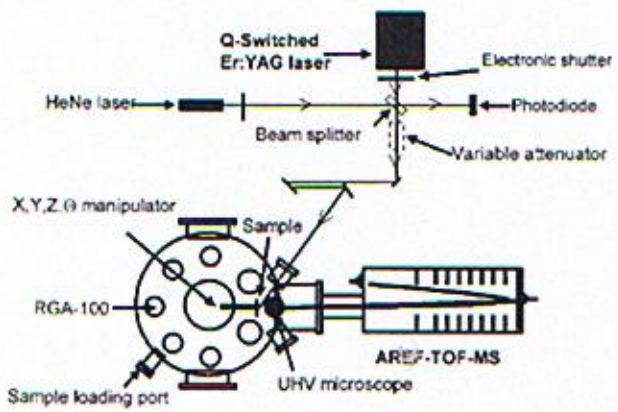

FIG. 1. Schematic drawing of experimental setup.

All of the CaF_2 samples measured in this work were obtained from St. Gobain/Bicron. The samples were cut at different orientations: 0°, 5°, 10°, and 15° off the (100) orientation, respectively, in order to measure the effect of curved surfaces in actual photolithographic stepper optics. All the samples were mechanically polished by the manufacturer at the same time. Removal of polishing residue form the GaF_2 surface was first done with a soapy water rinse and dried with a tissue, then the samples were wiped clean with methanol and acetone (1:1) moistened tissue. The samples were examined under optical microscope and no particles were seen on the surface. Prior to mounting in the UHV chamber, the samples were stored in a vacuum desiccator.

Each sample was mounted in a holder with a 1-cm-thick Pyrex glass behind it acting as an absorber. The sample holder was loaded into the vacuum chamber via a sample transfer rod onto a mechanical manipulator (Vacuum Generators, model HPT-RX) with X, Y, Z, and Θ control. The pressure in the UHV chamber was 1×10^{-10} Torr after bake out and maintained at $\leq5\times10^{-10}$ Torr after repeatedly loading and unloading the samples. The timing between the firing of the laser and ionization of desorbed neutral species was adjusted to obtain the maximum signal. Angular reflectron TOF was used to eliminate the effect of random background ions.[13]

III. RESULTS AND DISCUSSION

A. Qualitative results

With the current experimental setup, no signal was detected when the electron beam was turned off, indicating that the laser was not ionizing the desorbed molecules. The optimum electron beam emission current for ionization was found to be 0.5 mA at 60 eV and further increasing the current did not improve the LID signal. Qualitative measurements were performed at medium laser fluence (2.5 J/cm^2). A sequence of n laser pulses irradiated each site at a fixed laser fluence. As shown in Fig. 2, the ion intensity decreased with an increasing number of laser pulses. The first pulse always gave the highest ion intensity with ion intensity decreasing rapidly on subsequent pulses. In most cases, no peak was seen after five pulses, suggesting that the surface contaminants were being removed and little or no readsorption occurred between consecutive laser pulses.

From Fig. 3, one can see that the concentration (represented by the peak value of the LID signal) and types of contaminants (represented by the mass to charge ratio of the ion) on the (100) CaF_2 surface varied widely from site to site. For example, at site 1 the dominant peak was from water ions H_2O^+($m/z=18$) and only very small hydrocarbon

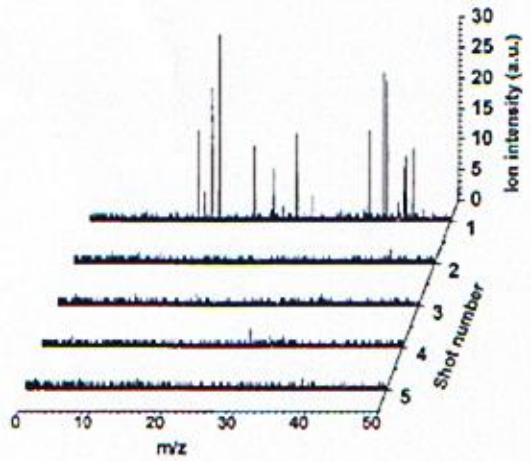

FIG. 2. LID TOF mass spectra of CaF_2 surface at different laser shots. The peak laser fluence is 2.5 J/cm^2. CaF_2 sample orientation is (100).

ion peaks (m/z=43, 44 and 45) were seen. While at site 2 the majority of peaks were hydrocarbon ions $C_xH_y^+$ and oxygen-containing hydrocarbon ions, such as CH_2O^+ and $C_2H_4O^+$ (m/z=30,44). It is impossible to specify the exact hydrocarbon composition because of the lack of intact molecular ions. The highest mass in spectrum (b) indicates that hydrocarbon molecules containing at least seven carbon atoms were adsorbed on the CaF_2 surface at this site. Water ions OH^+ and H_2O^+(m/z=17,18) appeared at lower intensity than the hydrocarbon ions at site 2. The alkali metal ions Na^+ and K^+ that were also found at site 2 were probably from physical contact with human skin during sample handling.

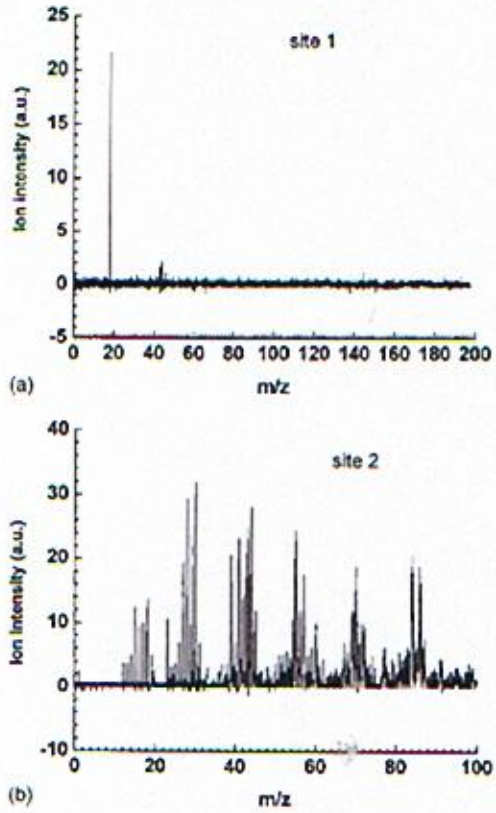

FIG. 3. LID TOF mass spectra of CaF_2 (100) at two different sites.

B. Determination of the LID threshold

Previous LID experiments showed[15–17] that a threshold laser fluence must be reached before desorption may occur. For a gaussian beam profile, as the laser fluence increases, the area of the surface heated above threshold also increases; the desorption yield increases, and it is possible to measure the dependence of desorption on the laser fluence.[15] To quantitatively analyze the LID data, a degenerate threshold model[11] was employed. This model assumes that adsorption occurs preferentially at surface defects and that there is a sharp increase in LID signal from a particular type of defect above the "threshold" laser fluence. According to the model, the desorption signal ψ for a particular defect is related to the peak laser fluence ϕ_0 by the following equation:

$$\Psi = m\pi\frac{\rho^2}{\cos\theta}(\ln\phi_0 - \ln\phi_{\text{th}}), \tag{1}$$

where ρ is the $1/e$ radius of the gaussian laser spatial distribution, θ is the incident angle of the laser beam, which is 60° in this work, ϕ_{th} is the LID threshold, and m is a proportionality parameter, which contains information on the defect density and adsorbate concentration. It is assumed that m is constant over the irradiated spot size. One can see that ϕ_{th} can be calculated from the zero intercept of total desorption signal, ψ versus $\ln(\phi_0)$.

In order to obtain the relationship between desorption signal and laser fluence when the concentration and type of contaminants on the CaF_2 surface varied from site to site, a N-on-one $[N(\phi_0)/1]$ test was used. Starting from the lowest laser energy where no signal was obtained, the laser energy was gradually increased at each new site on the surface. At each energy, five nominally identical pulses were used. The maximum laser fluence used was 7.0 J/cm^2, corresponding to a power intensity of 70.0 MW/cm^2, which is much lower than the multiple-shot damage threshold of CaF_2 crystal reported in the literature, $\sim 10^4$ MW/cm^2.[18] At each ϕ_0 the ion intensities of OH^+ and H_2O^+ were summed cumulatively from the lowest laser fluence to ϕ_0 in order to calculate the total desorption signal for water and hydrocarbons $[C_xH_y^+(x=1-4, y=0-2n+1)]$. The plot in Fig. 4(a) shows a simple straight line for water and hydrocarbons, implying a single class of defects, with ϕ_{th} (water) $\approx$1.0 J/cm^2 and ϕ_{th} (hydrocarbon) $\approx$1.5 J/cm^2. The plot in Fig. 4(b) shows two straight lines for each type of contaminant, implying two different types of defects. An initial desorption comes from defects with a relatively low threshold (ϕ_{th1} is $\sim$0.6 J/cm^2 for water and $\sim$0.5 J/cm^2 for hydrocarbons). At higher laser fluences, desorption from a second type of defect with a higher threshold (ϕ_{th2} is $\sim$2.2 J/cm^2 for water and $\sim$2.3 J/cm^2 for hydrocarbons) is added. The lower LID threshold in the zero intercept of the first line and the second

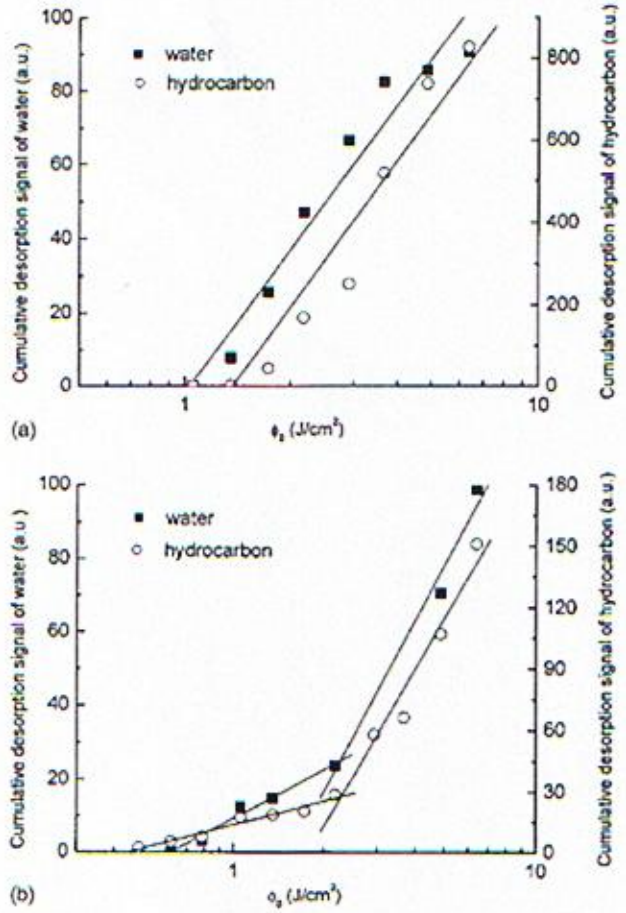

FIG. 4. Cumulative desorption signal of water and hydrocarbon ions as a function of peak laser fluence for $N(\phi_0)/1$ experiments on two different sites of CaF_2 (100) sample.

LID threshold is the zero intercept of the second line after subtracting the first line from the second line, i.e., the peak laser fluence at the intersection of first line and second line. Particular defects that result in the measured behavior have not yet been identified. The values of ϕ_{th} for water at 2.94 μm, 0.6 J/cm^2, and 2.2 J/cm^2, are one order of magnitude lower than the desorption thresholds reported at 2.7 μm, 4.7 J/cm^2, and 23 J/cm^2.[19] The difference is consistent with the fact that the absorption coefficient of water at 2.94 μm ($\varepsilon_{2.94\ \mu m}=1.22\times10^4$ cm^{-1}) is one order of magnitude higher than at 2.7 μm ($\varepsilon_{2.7\ \mu m}=0.74\times10^3$ cm^{-1}).[5] This indicates that 2.94 μm is more efficient at removing surface adsorbed water without damaging the underlying CaF_2 surface.

Hydrocarbons and water are presumably co-adsorbed or incorporated into surface defects during the polishing and cleaning operations. In most cases, the total desorption signal of hydrocarbons was larger than water. However, it cannot be concluded that the concentration of hydrocarbons is higher than water, as it is well known that the electron impact ionization efficiency of hydrocarbons is much greater than that of water. If the hydrocarbon ions originated from alcohol, the O–H group in alcohol would absorb light at $\lambda=2.94$ μm almost as efficiently as water. If the hydrocarbon ions originated from other organic molecules without an OH group, desorption would occur predominantly through the heating of water, as non-OH hydrocarbons do not have strong absorption at 2.94 μm. Both mechanisms could contribute to the similarity between hydrocarbon and water desorption behavior shown in Fig. 4.

C. Desorption thresholds at different orientation planes

For lenses in photolithography tools, a potential complication arises because of the curved surfaces involved. Therefore, it is important to look at surfaces that deviate from the (100) cleavage plane. The same LID experiments were carried out on different surface orientations: 0°, 5°, 10°, and 15° off the (100) orientation. The desorption threshold for water was measured and preliminary data showed that the values of the threshold varied largely from site to site on 0°, 5°, and 10° off-axis (100) samples, but for the 15° off-axis (100) sample, the variation is less and the average threshold is lower. Similar results were also found for hydrocarbon ions. As it is assumed that contaminants are preferentially adsorbed at surface defects, the variation of desorption thresholds would reflect the difference between defect structures of the surfaces. A large variation of desorption thresholds may suggest a large variation in defects existing on the surface while a smaller variation may suggest more uniformity in defects. Surface nanotopography was measured using an atomic force microscopy. The root mean square roughness (R_{rms}) values of a scan size 20×20 μm were measured to be 0.2–0.6 nm, 0.25–0.65, 0.25–0.68, and 0.56–0.75 nm for 0°, 5°, 10°, and 15° off the (100) orientation, respectively. Because we could not probe the same site on LID and AFM in the current experimental setup, no correlation between the desorption threshold and surface nanotopography can be drawn at this time.

D. Question: Are we damaging the surface?

One of the most important questions concerning laser cleaning is, Are we damaging the surface? In our experiment, efforts have been made to avoid laser damage of the surface: (1) The peak laser fluence used in LID was kept below the damage threshold values for mechanically polished CaF_2 reported in the literature, which are 15 J/cm^2 for multiple 248 nm/14 ns irradiations[20] and 30 J/cm^2 for single 248 nm/14 ns irradiation,[21] respectively. (2) A laser pulse width of ~100 ns instead of ~10 ns was used to avoid surface damage. At a pulse width of 100 ns, the damage threshold is expected to be higher than at 14 ns according to the generally accepted scaling rule that damage threshold increases linearly with the square root of the pulse length.[22] Brand and George[17] pointed out that there are significant advantages to using a longer pulse width (e.g., 100 ns) to reduce laser induced surface damage during laser induced thermal desorption. This argument is based on the fact that desorption requires a certain amount of time. Using a pulse

length shorter than the characteristic desorption time means that a higher peak power and, therefore, high peak temperature is required for desorption, producing a greater probability of stress damage. (3) LID experiments started from the lowest laser fluence. It has been reported that the surface damage threshold increased for experiments starting at low fluences (N/1), presumably because surface contaminants were removed at subdamage fluences.[23,24]

The CaF_2 surfaces were examined using both dark field and differential interference contrast microscopy after LID. No surface damage, such as craters, cracks, etc., was seen. However, in a very few cases during laser desorption, one could see some ion signals at m/z =59 (CaF^+), 137 (CaF_2CaF^+). It is believed that these signals were not due to the ablation of the bulk surface, but were from asperities in the already damaged surface layer produced during polishing, which remained on the surface after cleaning.[20] No such signals were seen in the LID experiments shown in Figs. 2–4. The absorption of CaF2 samples were measured on a UV-visible spectrometer before and after laser irradiation and no obvious change on the absorption was found from 190 nm to 800 nm.

IV. CONCLUSION

A laser induced desorption, electron impact ionization, time-of-flight mass spectrometer (LID-EI-TOFMS) was developed to study adsorbed molecular contaminants on critical optical surfaces, such as CaF_2. Water, hydrocarbone, oxygen-containing hydrocarbons as well as alkali ions (Na^+,K^+) were detected on CaF_2 (100) surfaces. For multiple irradiations of one site, the ion intensities decreased as the pulse number increased, suggesting that the surface was being cleaned. A degenerate threshold model that assumed preferential adsorption at surface defects was employed to quantitatively analyze the LID data. Desorption thresholds for water and hydrocarbons were obtained from this model. The concentration and type of contaminants on the CaF_2 surfaces varied from site to site. The desorption threshold also varied from site to site for 0°, 5°, 10° off-axis (100) samples, but for the 15° off-axis (100) sample, the variation was less and the average threshold was lower.

ACKNOWLEDGMENTS

This work is sponsored by DARPA Grant No. F33615-00-1-1727. The authors wish to thank DARPA, in general, and Dave Patterson, in particular, for supporting this work. We also wish to thank G. David Via of WPAFB. We are grateful to St. Gobain/Bicron for providing CaF_2 samples for analysis and for technical advice and discussion. Also, thanks to the Department of Physics machine shop of Florida State University, and to Ian Winger in particular, for the design and construction of the sample mounting system. Patrick Davis provided great help in setting up the instruments.

[1]W. Zapka, W. Ziemlich, and A. C. Tam, Appl. Phys. Lett. **58**, 2217 (1991).
[2]W. Zapka, A. C. Tam, and W. Ziemlich, Microelectron. Eng. **13**, 547 (1991).
[3]V. Liberman, T. M. Bloomstein, M. Rothschildd, J. H. C. Sedlacek, R. S. Uttaro, A. K. Bates, C. V. Peski, and K. Orvek, J. Vac. Sci. Technol. B **17**, 3273 (1999).
[4]V. M. Bermudez, Appl. Surf. Sci. **161**, 227 (2000).
[5]M. R. Querry, D. M. Wieliczka, and D. J. Segelstein, in *Handbook of Optical Constants of Solids II*, edited by E. D. Palik (Academic, San Diego, CA, 1991), pp. 1059–1077.
[6]S. I. Kudryashov and S. D. Allen, J. Appl. Phys. **92**, 5159 (2002).
[7]S. I. Kudryashov and S. D. Allen, J. Appl. Phys. **92**, 5627 (2002).
[8]T. M. Bloomstein, M. Rothschild, R. R. Kunz, D. E. Hardy, and R. B. Goodman, J. Vac. Sci. Technol. B **16**, 3154 (1998).
[9]T. M. Bloomstein, M. Rothschild, V. Liberman, D. Hardy, N. N. Efremow Jr., and S. T. Palmacci, Proc. SPIE **4000**, 1537 (2000).
[10]G. Holler, U. Albecht, S. Herminghaus, and P. Leiderer, Appl. Phys. Lett. **62**, 2877 (1993).
[11]S. D. Allen, J. O. Porteus, W. N. Faith, and J. B. Franck, Appl. Phys. Lett. **45**, 997 (1984).
[12]R. K. Shori, A. A. Walston, O. M. Stafsudd, D. Fried, and J. T. Walsh, Jr., IEEE J. Sel. Top. Quantum Electron. **7**, 959 (2001).
[13]S. D. Allen, J. M. Fu, Y. Surapaneni, A. J. Hopkins, and P. S. Davis, Proc. SPIE **4977**, 1 (2003).
[14]S. Kano, S. C. Langford, and J. T. Dickinson, J. Appl. Phys. **89**, 2950 (2001).
[15]R. B. Hall and A. M. Desantolo, Surf. Sci. **137**, 421 (1984).
[16]S. M. George, in *Physical Methods of Chemistry*, 2nd ed., Vol. IXA Investigations of Surface and Interfaces-Part A, edited by B. W. Rossiter and R. C. Baetzold (Wiley, New York, 1986), Chap. 7, p. 453.
[17]J. L. Brand and S. M. George, Surf. Sci. **167**, 341 (1986).
[18]A. Rosenfeld, M. Lorenz, R. Stoian, and D. Ashkenasi, Appl. Phys. A: Mater. Sci. Process. **69**, S373 (1999).
[19]J. O. Porteus, J. B. Franck, S. C. Seitel, and S. D. Allen, Opt. Eng. **25**, 1171 (1986).
[20]H. Johnsen and G. Kastner, J. Mater. Sci. **33**, 3839 (1998).
[21]S. Gogoll, M. Reichling, J. Sils, H. Johnsen, and E. Matthias, Appl. Phys. A: Mater. Sci. Process. **69**, S743 (1999).
[22]A.-C. Tien, S. Backus, H. Kapteyn, M. Murnane, and G. Mourou, Phys. Rev. Lett. **82**, 3883 (1999).
[23]S. D. Allen, J. O. Porteus, and W. N. Faith, Appl. Phys. Lett. **41**, 416 (1982).
[24]I. Laidler and D. C. Emmony, NBS Spec. Publ. **746**, 182 (1987).